Theoret. Chim. Acta (Berl.) 49, 161–181 (1978)

THEORETICA CHIMICA ACTA

An *ab initio* Theoretical Study of the Binding of Zn^{II} with Biologically Significant Ligands: CO_2, H_2O, OH^-, Imidazole, and Imidazolate

Daniel Demoulin and Alberte Pullman

Institut de Biologie Physico-Chimique, Laboratoire de Biochimie Théorique associé au C.N.R.S., 13, rue P. et M. Curie, F-75005 Paris, France

Zinc is one of the most important biological metals involved in the catalytic site of many enzymes. SCF *ab initio* computations with good quality basis sets are reported for monoadducts of Zn^{II} with various biologically significant ligands, and the fundamental features of the binding are characterized, using in particular energy decomposition scheme, population analysis and difference density curves. A test of the possibility of using pseudopotentials in this domain is also reported.

Key words: Zn^{II} complexes (*ab initio* study) – Catalysis

1. Introduction

Zinc is one of the most important and most ubiquitous biological metals. Its better-known involvement is its presence at the catalytic site of many enzymes. In those of known structure it is often found in a more or less distorted tetrahedral environment, with histidines and water (or OH^-) among the ligands [1]. Among these are carbonic anhydrase [2] (one water, three histidines), carboxypeptidase [3] and thermolysine [4] (one water, one glutamate, two histidines) and liver alcohol dehydrogenase [5] (one water, two cysteines and one histidine). Enzyme-bound zinc is an essential component of many DNA- [6, 7] and RNA- [8, 9] polymerases. The role of zinc in normal and leukemic leucocyte metabolism has been underlined recently [10]: quoting from Ref. [10] "Zinc is essential for the growth of all species. Growth arrest results from its deficiency and presumably reflects important roles of this metal at critical points of metabolism . . . The biological essentiality of zinc can be discerned at various steps of cell growth and development in both normal and neoplastic cells". We have thus deemed it worthwhile to start a large-scale quantum-chemical study of the interactions of

0040-5744/78/0049/0161/$04.20

Zn^{++} with various biological molecules [11]. Aside from its pure theoretical interest, a detailed analysis of the intrinsic nature of the binding between zinc and its various ligands represents a necessary first step towards an understanding, at the molecular level, of the biological role(s) of the zinc ion.

Very few theoretical studies of zinc compounds have been performed up to now. At the *ab initio* level, most previous calculations involving Zn deal with simple inorganic compounds such as zinc sulfide [12] or chloride [13, 14] or $Zn(CH_3)_2$ [15]. Very recently, calculations were performed on complexes of zinc with $C_2H_2X_2$ compounds for X = NH, S, O [16].

In the presently reported work we concentrate on the ligands imidazole (ImH), water (OH_2), carbon dioxide (CO_2) and the anions imidazolate (Im^-) and hydroxyl (OH^-). In a preliminary report [11] we have centered our attention on two problems raised in connection with the possible mechanism of action of carbonic anhydrase, namely a) the effect of zinc-binding on the ease of deprotonation of its ligands water and/or imidazole [17], b) the ability of CO_2 (the substrate of the enzyme) to bind to zinc as a more or less distant ligand [18]. It was shown that whereas free imidazole is less difficult to ionize than free water (in agreement with experiment), binding to the cation strongly facilitates the process for both species, but in such a way as to reverse the order, zinc-bound water being more easily ionized than zinc-bound imidazole. On the other hand, binding of CO_2 to Zn^{++} was found possible although less favorable than that of the other ligands studied. The implications of these results on the possible mechanism of action of carbonic anhydrase are being currently studied and will not be further dealt with here. In the present paper we concentrate merely on the fundamental aspects of the binding of Zn^{++} to the various ligands studied, discussing in particular the general nature of the binding and its variation according to the ligand, with the help of an energy decomposition scheme [19], of Mulliken population analysis [20] and of electron density difference plots. Furthermore in the final part of the paper, we utilize the results of our all-electron *ab initio* computations to test the possibilities, in this field, of valence-electrons-only computations using a recently developed pseudopotential technique [21, 22].

2. Method, Geometries and Basis Sets

In order to avoid the doubts bound to the utilization of semi-empirical methods in a relatively unexplored field, we have chosen to work at the *ab initio* level. The complexes were treated as supermolecules using the SCF closed-shell molecular orbital method. The correlation correction to the SCF computed enthalpy of cation binding has been explicitly computed in the case of the system $Li^+ \cdots H_2O$ [23, 24] where it does not reach over 3 percent of the total binding energy. A GVB evaluation [25] in the case of $Li^+ \cdots NH_3$ and $Li^+ \cdots OH_2$ indicates a correction of about 1 kcal/mole to the binding energies (40 and 36 kcal/mole respectively). Moreover a very recent calculation [26] of the systems $Mg^{++} \cdots H_2O$ and $Ca^{++} \cdots H_2O$ yields correlation corrections of about 2 and 5% respectively. One may hope that the correlation correction in the case of Zn^{++}

complexes remains in a similar range. At any rate, an SCF computation is a prerequisite to the evaluation of any correction to it and to an approximate understanding of the nature of the binding.

The geometries of the ligands were taken from the literature [27–29] except for OH^- where the OH distance was optimized, yielding $d_{OH}=0.98$ Å. A compilation of structures of imidazole and histidine transition metal complexes, made by Freeman [30] and recently extended [31], having shown that the bond distances in the complexed imidazole ring, be it neutral or anionic, do not vary much from those in the free ligand, we have adopted the experimental geometry of imidazole crystals for both ImH and Im^-. The bond lengths and angles utilized are summarized in Fig. 1.

In all computations on the Zn^{++}···ligand complexes the geometry of the ligand was kept frozen. For every complex, the distance Zn^{++}···ligand was optimized first, then angular distortion (θ, see Fig. 1) was allowed at the equilibrium distance. The approach of the cation was made as follows: for CO_2 towards the oxygen along the CO axis; for H_2O, towards the oxygen along the bisectrix of the HOH angle, for OH^- towards the oxygen along the HO axis; for imidazole towards the nonprotonated nitrogen atom, along the bisectrix of the CNC angle, the same disposition being kept for the approach to the imidazolate anion.

Gaussian basis sets taken from the literature ([32] for Zn, [33] for the first-row atoms and [34] for hydrogen) have been suitably modified to yield the basis of Table 1, obtained as follows: for the Zn cation, as in Ref. [16], we deleted from the original basis the *s*, *p*, and *d* function of highest exponent, and also the three *s* functions of lowest exponents which become redundant when suitable *d* functions are present; this remaining zinc basis was supplemented by a set of diffuse *p* and *d* functions ($\zeta=0.2534$ and 0.2313 respectively) to insure a good description of the 3*d*, 4*s*, and 4*p* orbitals. (The utilization of two diffuse *p* functions of $\zeta=0.4221$ and 0.1521 instead of one only of $\zeta=0.2534$, led to an overrepresentation of the cation

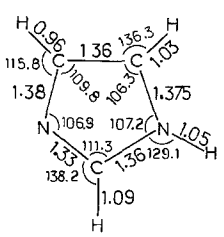

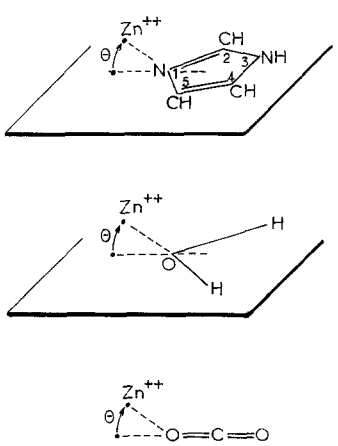

Fig. 1. Geometrical parameters and atom numbering

with respect to the ligands in the basis set chosen, hence to a spurious charge transfer in tests performed for $Zn^{++}\cdots OH_2$ and $Zn^{++}\cdots OH^-$.) The final 8*s*; 6*p*; 4*d* functions for the cation were contracted as 5,2,1 for *s*, 3,1,1,1 for *p* and 2,1,1 for *d* with the coefficients given in Table 1. With this basis, the totally symmetric combinations of our *d* functions (XX+YY+ZZ) form *s* functions of maximum radial amplitude appropriate to describe the Zn 3*s* and 4*s* atomic orbitals. Thus the final basis is equivalent to a 12*s* basis contracted into 6 functions.

For oxygen we tested the Whitman–Hornback (8*s*, 4*p*) basis [35] and the Roos–Siegbahn (7*s*, 3*p*) one, both contracted into 3*s* and 2*p* functions, and obtained essentially similar results for the complex $Zn^{++}\cdots H_2O$. Thus the (7*s*, 3*p*) basis was

Table 1. Final Gaussian exponents α and contraction coefficients c

	α	c		α	c
Zinc			Hydrogen		
s	12711.4	0.01277	*s*	19.24056	0.01906
	2919.19	0.06254		2.899152	0.13424
	836.851	0.21289		0.653410	0.47449
	277.916	0.43842		0.177576	1.0
	100.822	0.38157	Nitrogen		
	26.4643	0.42031	*s*	2038.41	0.004479
	11.2290	0.67925		301.689	0.034581
	3.03908	1.0		66.4630	0.164263
p	140.104	0.15575		17.8081	0.453898
	43.8249	0.45184		5.30452	0.468979
	15.4003	0.48964		0.764993	1.0
	4.24035	1.0		0.234424	1.0
	1.33289	1.0	*p*	5.95461	0.119664
	0.2534	1.0		1.23293	0.474629
d	9.05781	0.30021		0.286752	1.0
	2.73823	0.51677		0.067	1.0
	0.731228	1.0	Carbon		
	0.231293	1.0	*s*	1412.29	0.004813
Oxygen				206.885	0.037267
s	2714.89	0.004324		45.8498	0.172403
	415.725	0.032265		12.3887	0.459261
	91.9805	0.156410		3.72337	0.456185
	24.4515	0.447813		0.524194	1.0
	7.22296	0.481602		0.163484	1.0
	1.06314	1.0	*p*	4.18286	0.112194
	0.322679	1.0		0.851563	0.466227
p	7.75579	0.129373		0.199206	1.0
	1.62336	0.481269			
	0.36503	1.0			
	0.08	1.0			

adopted. However the description of OH^- required the addition of a diffuse *p* function, otherwise the orbital energies of the lone pairs were nearly zero. Optimization of the exponent of this *p* function on OH^- led to $\zeta = 0.08$. The final 7*s*, 4*p* set of Gaussians was used for both H_2O and OH^- in all computations with the contraction given in Table 1 (5,1,1 for *s* and 2,1,1 for *p*).

Upon addition of the diffuse *p* function above, the proton affinity of OH^- calculated as $\mathscr{E}(OH_2) - \mathscr{E}(OH^-)$ drops from 441.5 to 392.1 kcal/mole. The experimental value is 390 kcal/mole [36]. Without putting too much emphasis on this agreement, one may however take it as an indication that the basis set is satisfactory. Concerning the binding to the cation, the addition of a diffuse *p* function on oxygen does not bring about significant variations in the optimum geometry of the complexes $Zn^{++}\cdots OH_2$ or $Zn^{++}\cdots OH^-$, nor in the shape of the potential curves, but the binding energy of Zn^{++} to OH^- goes from -461 to -410 kcal/mole. That of the neutral species OH_2 is little affected, decreasing from -112.4 to -104 kcal/mole only. For this last reason the computations on CO_2-binding were performed without the diffuse *p* function on the ligand.

For nitrogen in imidazolate, the same situation arises as in OH^-. Thus exponents for diffuse *p* functions on nitrogen and carbon were chosen, by comparison with the oxygen case (0.067 for N and 0.047 for C). Test computations were performed for four reactions involving ImH and Im^- with these diffuse functions on both C and N or on N only (Table 2). The energy differences obtained never exceeded 1.5%. On this basis and after detailed examination of the results for Im^- (the most sensitive test) we decided not to use diffuse *p* functions on the carbon atoms, but only on the nitrogens of the imidazole cycle.

Although the diffuse *p* functions are needed to obtain a good description of the anions, it must be emphasized that their higher occupied molecular orbitals are by no means diffuse: for example the size of the highest (π) MO in the imidazole anion and in imidazole itself are very similar when measured by $\langle Z^2 \rangle$ the second moment of the charge distribution perpendicular to the molecular plane ($\langle Z^2 \rangle = 2.236$ and 2.195 $(a.u.)^2$ respectively).

Table 2. Computed energies (kcal/mole) with (A) and without (B) a diffuse *p* function on carbon, for reactions involving ImH and Im^-

Reaction	A	B
$ImH \rightarrow Im^- + H^+$	367.5	371.0
$Zn^{++}\cdots ImH \rightarrow Zn^{++}\cdots Im^- + H^+$	166.6	169.1
$Zn^{++}\cdots Im^- \rightarrow Zn^{++} + Im^-$	365.6	367.8
$Zn^{++}\cdots ImH \rightarrow Zn^{++} + ImH$	164.7	165.8

3. Results and Discussion

The binding energies for the complexes studied are given in Table 3 for all the geometries considered. It is seen that the bond strength with the three neutral ligands is appreciable, ranging at equilibrium from 80 kcal/mole for CO_2, to 170 kcal/mole for imidazole, with an intermediate value for water; while the binding of the anions imidazolate and hydroxyl reach up to 370 and 410 kcal/mole respectively. (The presence or absence of diffuse p functions on the ligand although modifying somewhat the binding energies does not affect this ordering (see Table 4).)

We do not know of any experimental gas-phase binding energy for the present complexes to which our computed values could be compared. Theoretical calculations by Veillard *et al.* [37] on $Cu^{++}\cdots OH_2$, with comparable although not identical basis sets, gave a binding energy of 115 kcal/mole at an equilibrium distance of 1.84 Å (to be compared to our value for $Zn^{++}\cdots OH_2$ of 112.9 kcal/mole at $R=1.89$ Å). Infrared spectroscopy experiments on cation hydrates at low degree of hydration [38] indicate a great similarity between the Cu^{++} and Zn^{++} monohydrates, hence supporting the similarity found in the theoretical values.

Our computed bond lengths for the various ligands fall between 1.82 and 1.90 Å. Taking into account the fact that the cation–ligand equilibrium distance increases upon increasing the number of bound ligands, the computed values compare well with the 2.0 Å distance usually found in crystals [30, 31, 39, 40] where Zn^{++} has several ligands. The shorter length found for $Zn^{++}\cdots OH^-$ seems due to the small size of the ion, allowing a closer approach.

The most favorable geometry of all the complexes (with the possible exception of $Zn^{++}\cdots OH^-$) occurs for $\theta=0$. However, the $Zn^{++}\cdots L$ bond, while strong, appears easy to distort: stretching by 0.10 Å, or bending up to 30° is achieved at the cost of only a few kcal/mole, a small percentage of the total bond energy. Bending is easiest with the anionic ligands and the optimal angle in $Zn^{++}\cdots OH^-$ appears slightly different from zero. This angular lability appears supported by structural data indicating angles θ up to 30° in imidazole complexes [30] and by the failure of attempts to synthetize sandwich imidazolate complexes analogous to the well-known cyclopentadienyl complexes [31].

3.1. The Nature of Zn^{++} Binding

The bond strength for the ligands considered increases in the order $CO_2 < OH_2 < ImH < Im^- < OH^-$. Qualitative electrostatic considerations would indicate the same ordering, since CO_2 has only a quadrupole moment, ImH has a larger dipole moment than OH_2 (4.02 [41] vs. 1.85 debyes [42]) and Im^- and OH^- bear a negative charge. A simple evaluation using the experimental quadrupole moment and polarizability of CO_2 [43] gives an interaction energy of -70.5 kcal/mole at the calculated optimal Zn···O distance of 1.85 Å (-39.4 kcal/mole for the charge-quadrupole term and -31.1 kcal/mole for the polarization term).

These qualitative evaluations may be compared with the results of a theoretical decomposition of our calculated binding energies into components [19] (Table 4):

Table 3. Computed binding energies to Zn^{++} of various ligands at various distances and angles

Complex	R, Å	θ, Deg	ΔE[a]	$\delta(\Delta E)$[b]
$Zn^{++}\cdots OCO$[c]	1.8	0		0.5
	1.85	0	−79.4	0.0
	1.9	0		0.5
	2.0	0		3.5
	2.1	0		8.2
	2.3	0		19.3
	2.5	0	−48.9	30.3
	1.85	15		1.1
	1.85	30		4.7
	1.85	60		22.93
$Zn^{++}\cdots OH_2$	1.8	0		1.37
	1.89	0	−104.1	0.0
	2.0	0		2.34
	1.89	15		1.22
	1.89	30		4.95
	1.89	60		20.78
	1.89	90		50.43
$Zn^{++}\cdots ImH$	1.8	0		1.10
	1.87	0	−169.4	0.0
	1.9	0		0.26
	2.0	0		3.46
	2.1	0		9.13
	1.87	15		1.75
	1.87	30		6.72
	1.87	60		24.62
$Zn^{++}\cdots Im^{-}$	1.65	0		9.49
	1.75	0		1.10
	1.82	0	−366.4	0.0
	1.85	0		0.42
	1.95	0		4.63
	1.82	15		0.91
	1.82	30		3.40
	1.82	60		12.05
$Zn^{++}\cdots OH^{-}$	1.55	0		12.06
	1.65	0		0.96
	1.70	0	−410.7	0.0
	1.75	0		1.23
	1.70	15		−0.04
	1.70	30		+0.06
	1.70	60		4.09
	1.70	90		21.34

[a] ΔE: binding energy (kcal/mole) of $Zn^{++}\cdots L$, computed as $E(Zn^{++}\cdots L) - E(Zn^{++}) - E(L)$.

[b] $\delta(\Delta E)$: energy with respect to optimum geometry (kcal/mole).

[c] No diffuse p functions were used on the neutral CO_2 ligand. Calculations on $Zn^{++}\cdots OH_2$ without diffuse p functions on OH_2 give a ΔE of −112.8 kcal/mole, and the same equilibrium geometry as that obtained with the diffuse p function.

The following energies were obtained for the fragments (in hartrees): Zn^{++} −1767.86981, CO_2 −187.17985, OH_2 −75.85642, ImH −224.34285, Im^{-} −223.75396, OH^{-} −75.23160.

Table 4. Decomposition of the binding energy in the most stable linear complexes (energies in kcal/mole)

Ligand	R(Å)[c]	ΔE	E_C	E_{EX}	E_{DEL}
CO_2[a]	1.85	−79.4	−55.1	34.5	−58.9
H_2O[a]	1.89	−112.9	−100.2	33.4	−46.1
ImH[a]	1.87	−172.0	−149.6	69.7	−92.1
H_2O[b]	1.89	−104.2	−115.9	47.4	−35.6
ImH[b]	1.87	−169.5	−170.1	85.8	−85.1
Im^-[b]	1.82	−366.4	−391.0	123.9	−99.3
OH^-[b]	1.70	−410.8	−452.6	113.5	−71.7

[a] Without diffuse p orbitals on the ligand O or N atoms.
[b] With diffuse p orbitals on the ligand O or N atoms.
[c] R(Å): equilibrium distance; ΔE and components (kcal/mole) as defined in the text.

a Coulombic term E_C, calculated as the Coulomb interaction of the charge cloud and nuclei of fragment A with those of fragment B supposed unperturbed; an exchange term, repulsive, E_{EX} due to the Pauli-principle repulsion between electrons of A and electrons of B; and a polarization + charge-transfer term, called also delocalization term E_{DEL}, which accounts for the modifications of the electron cloud of fragment A by the electric field of fragment B and vice versa. (We have chosen not to separate the charge transfer and polarization terms [44] because their sum is less basis-set dependent than each of them separately. In any case, energy components are not variationally determined quantities, but we expect them to have at least comparative values.)

The Coulombic term E_C alone gives indeed the same ordering as the total binding energy. For $Zn^{++}\cdots OH_2$ and $Zn^{++}\cdots ImH$ (with diffuse p functions), $E_C \simeq \Delta E$. For the anionic ligands OH^- and Im^-, $|E_C| > |\Delta E|$ and the equilibrium distances are smaller than for the corresponding neutral ligands. This shorter distance and the greater extension of the sigma lone pairs of O or N in the anion lead to a higher repulsive exchange term E_{EX} and to a somewhat increased delocalization term. For CO_2, we do find that the Coulombic term E_C and the delocalization term E_{DEL} contribute about equally to the binding energy. The exchange repulsion is rather small, probably indicative of the small extent of CO_2's charge density. (In CO_2, the electron density falls at 10^{-4} e/a.u.^{3} at only 3.3 a.u. in front of the oxygen atom in the direction of the bond to be formed with zinc. In OH_2 and ImH this distance is slightly above 4.0 a.u. and in Im^- and OH^-, above 4.5 a.u.)

Although the separation into components varies upon addition of the diffuse p functions on the ligand, this does not change the general trends: leading Coulomb term for all complexes; upon ionization of the ligand increasing delocalization together with increased exchange in $OH_2 < ImH$. Note that E_{EX} increases as expected upon adjunction of the diffuse p function whereas E_{DEL} decreases and E_C increases.

Further information can be gained by considering the shifts in the electron distribution upon complexation. The result of a Mulliken population analysis is given in Table 5 in terms of charge transfer and charge shifts. The detailed atomic charge changes upon complex formation are given in Fig. 2 for Zn^{++}···ImH only. Charge gains and charge losses add up to zero; charge gains are partitioned into charge transferred to Zn^{++} and charge shift (internal charge transfer) i.e. the π charge transfer in Zn^{++}···ImH is 0.029 e while the π charge shift is $0.331+0.017=0.348$ e.

Again, relative values are of interest. Charge transfer increases in the order $CO_2<OH_2<ImH<OH^-<Im^-$, which, except for OH^-, is the order of increasing binding energy. However $-E_{DEL}$ (Table 4) increases in the order: $OH_2<CO_2<OH^-<ImH<Im^-$. This indicates that the polarization contribution in E_{DEL} is especially important for CO_2, ImH and Im^-. Indeed the charge shifts (Table 5) which one may qualitatively relate to the polarization energy term, are the largest for ImH and Im^-.

The charge shift on CO_2 is also quite large (twice that on OH_2) and much greater than the charge transfer. The charge shift is due to the π orbitals, while charge transfer arises mostly from σ orbitals (Table 5). This shows that the relatively large E_{DEL} for CO_2 (Table 4) is essentially due to the polarization contribution, due to the high polarizability of the molecule. It qualitatively agrees with the classical, electrostatic plus polarization model mentioned earlier.

Table 5. Mulliken population analysis (in 10^{-3} electron)

Ligand	R^c Å	θ Degree	Charge transfer to Zn^{++}				Charge shift on L		
			Total	σ	π	%π	Total	σ	π
CO_2[a]	1.85	0	194	150	44	23	281	—	288
		60	257	102	165	61	148	—	155
H_2O[a]	1.89	0	258	222	36	14	93	126	—
		60	312	119	192	62	—	186	—
ImH[a]	1.87	0	394	359	35	9	382	150	351
		60	438	262	176	41	290	202	260
H_2O[b]	1.89	0	207	183	24	13	149	171	—
		60	281	117	164	58	—	146	—
ImH[b]	1.87	0	351	322	29	8	414	163	348
		60	423	213	210	50	276	237	183
Im^-[b]	1.82	0	473	420	53	11	346	104	308
		60	563	247	316	56	203	270	75
OH^-[b]	1.70	0	397	247	150	38	—	52	—
		60	532	143	389	73	—	60	—

[a] Without diffuse p orbitals on the ligand O or N atoms.
[b] With diffuse p orbitals on the ligand O or N atoms.
[c] R equilibrium distance; θ: bond angle (Fig. 1), charge transfer and shift as defined in the text.

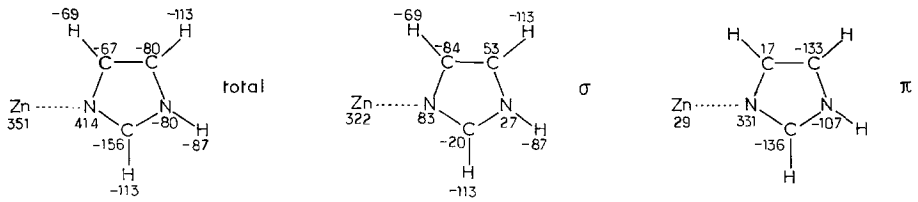

Fig. 2. Changes in atomic populations (10^{-3} e) upon complexation in Zn^{++}···imidazole. (Positive value = electron gain)

Another, perhaps more precise, image of the electron displacements upon Zn-binding is given by electron density difference plots obtained as $\rho_{\text{complex}} - \rho_{\text{separated ligands}}$ [45]. These plots present a set of common features clearly typical of the Zn^{++}···ligand bond, which are illustrated in Fig. 3 for OH_2, OH^-, and CO_2: disregarding the numerical differences and the small differences in the detailed shape of the curves, the binding to Zn^{++} can be characterized as follows: on the zinc ion, there is a zone of strong density increase on the atom and close to it on the Zn···L bond axis. This zone, appreciably larger on the internal side of the Zn···L bond than away from it, is surrounded by a zone of density depletion, which has its maximum on the axis on both sides of the Zn ion. Going towards the ligand atom L we find a zone of density increase, relatively weak on the Zn···L axis and prolongating an area of strong increase around and behind the L atom. This surrounds a zone of strong density decrease just in front of L on the Zn···L axis, indicative of electron transfer from the lone pair of L.

Going further away from Zn on the ligand molecule, a new zone of density depletion appears, then a zone of increased density on and behind the next atom, C of CO_2 or of imidazole; followed by a repetition of the same pattern along the next bonds as the distance to Zn increases. (Interestingly, from this point of view, one observes that an end atom carrying lone-pairs (O of CO_2 or N^- of imidazolate), behaves qualitatively as an end NH or CH or OH bond: depletion of the density in the far- (from Zn^{++}) region with piling-up of charge towards the "heavy" atom.) Along a bond situated nearly perpendicularly to the Zn–L axis (C–N of imidazole or imidazolate) the alternance depletion-enhancement of the density does not occur, the whole bond line being situated in the region of small density increase.

These density increases on the far atoms are located in the molecular plane, and are not due to π electron back-donation, as can be seen in Fig. 3d for Zn^{++}···OCO and even better in Fig. 4b, which shows the charge density difference in Zn^{++}··· ImH 1 a.u. above the molecular plane (the diagram for Zn^{++}···Im^- is very similar and not shown here).

At this stage, it is of interest to compare the density difference maps obtained for Zn^{++}···OH_2 and HOH···OH_2 using the same basis set. Figs. 3a and 3b show the density changes in the plane of the electron-donor water molecule. (The density changes in a plane perpendicular to the electron-donor water molecule show the

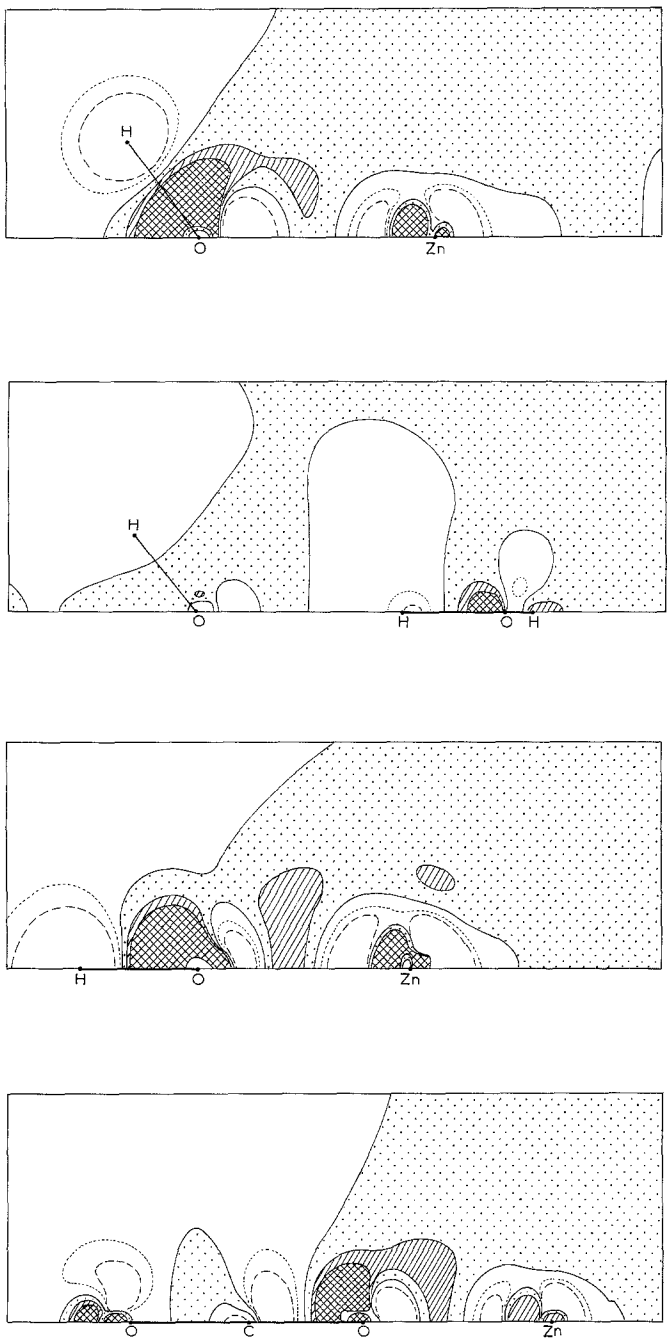

Fig. 3. Contours of isodensity differences in: **a)** $Zn^{++}\cdots OH_2$; **b)** $HOH\cdots OH_2$; **c)** $Zn^{++}\cdots OH^-$; **d)** $Zn^{++}\cdots OCO$. Density increases are indicated by various shadings: dotted: between 0.0 and 0.004 e/a.u.^{3}, hatching: between 0.004 and 0.007 e/a.u.^{3}, cross-hatching: above +0.007 e/a.u.^{3}. For density decreases, isodensity contours are shown: dotted line: −0.004 e/a.u.^{3}; dashed line: −0.007 e/a.u.^{3}; full line: zero density change

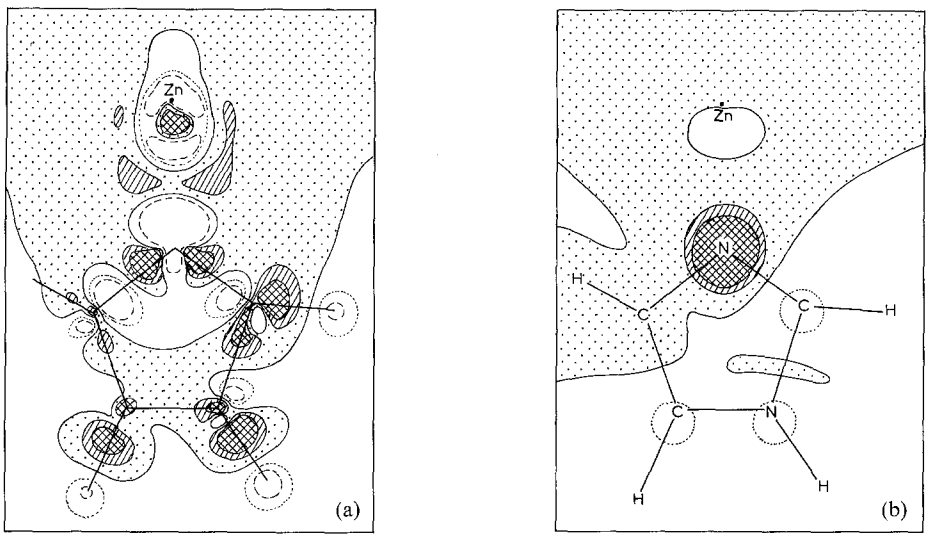

Fig. 4. Contours of isodensity differences in: **a)** Zn^{++}···ImH in the molecular plane; **b)** Zn^{++}···ImH 1.0 atomic unit above the molecular plane. Thresholds and conventions as in Fig. 3

same similarities and are not given here.) Comparison of H_2O···H_2O and H_2O···Zn^{++} binding characteristics points to a very similar *qualitative* behavior of the electron displacements upon hydrogen bonding and Zn–ligand binding; electron depletion in the lone-pair region, associated with a draining of charge towards the electron-losing oxygen, along the two HO bonds, at the expense of the hydrogens; slight gain of electrons in the "bond" region; and at the other end, the cation and the OH entities behave qualitatively in a similar way: depletion of the outer region, including H for OH, piling up of electrons close to the Zn or to the oxygen end of the OH bond and at their back, with another intermediate decrease in-between.

Similar features were observed in earlier studies of H bonding [45] [46], of Li^+ binding [47, 48], and more recently of charge-transfer complexing [49]. It appears that the characteristics observed are common features of all the interactions between closed-shell entities, only the details of the overall displacements differing according to the nature of the complex, that is the relative weights of the various components in the binding which is particularly visible in the intermediate "bond" region where the depleting effect of the exchange repulsion is more or less compensated by the accumulation due to charge transfer. In this respect the Zn^{++}···L bond appears intermediate between the hydrogen bond and the charge transfer complexes of Ref. [49].

3.2. Angular Dependence of the Binding

The energy decomposition scheme described above was used formerly [19] to discuss the angular dependence of the hydrogen bond energy in amide dimers.

Kollman [50] insisted on the role of the charge transfer component in H bonding, but came back recently to stress [51] the importance of the Coulomb term.

Let us consider the angular preference observed in our complexes in the light of the variation in the binding components (Table 6) and in the electron displacements (Table 5) upon varying θ from 0 to 60 degrees. We have found that all the complexes prefer $\theta=0$ (except OH^-, *vide supra*). Table 6 shows that the main factor which favors $\theta=0$ is the electrostatic component of the interaction energy (except in OH^- where E_C favors a large θ). On the contrary, E_{DEL} would favor $\theta\neq 0$ particularly for ImH and Im^-, this corresponding to a charge transfer allowed from the high-lying π molecular orbitals of the ligand to the empty 4*s* orbital of Zn^{++}, which can occur only when the σ–π symmetry is destroyed. Indeed we see in Table 5 that charge transfer to Zn^{++} increases with increasing θ, but the magnitude of the increase cannot be related to the magnitude of the energy change, which is rather small, except for ImH and Im^-.

All the complexes which prefer $\theta=0°$ do so for different reasons, and we may distinguish three groups:

For $Zn^{++}\cdots OCO$ and $Zn^{++}\cdots OH_2$, the loss of Coulomb energy as θ increases is accompanied by a small increase in exchange repulsion, not at all compensated by the small energy lowering due to increased polarization and charge transfer.

Table 6. Angular dependence of the binding energy and of its components (kcal/mole)

Ligand	R(Å)[c]	θ	ΔE	E_C	E_{EX}	E_{DEL}
CO_2[a]	1.85	60°	−56.5	−37.3	40.1	−59.3
		Δ(60°–0°)	22.9	17.8	5.6	−0.4
H_2O[a]	1.89	60°	−94.5	−82.6	36.8	−48.7
		Δ(60°–0°)	18.4	17.6	3.4	−2.6
ImH[a]	1.87	60°	−148.4	−111.3	63.4	−100.5
		Δ(60°–0°)	23.6	38.3	−6.3	−8.4
H_2O[b]	1.89	60°	−83.4	−99.2	53.3	−37.4
		Δ(60°–0°)	20.8	16.7	5.9	−1.8
ImH[b]	1.87	60°	−144.8	−125.7	76.0	−95.0
		Δ(60°–0°)	24.7	44.4	−9.8	−9.9
Im^-[b]	1.82	60°	−354.4	−352.8	109.0	−110.6
		Δ(60°–0°)	12.0	38.2	−14.9	−11.3
OH^-[b]	1.70	60°	−406.7	−489.1	155.6	−73.1
		Δ(60°–0°)	4.1	−36.5	42.1	−1.4

[a] Without diffuse *p* orbitals on the ligand O or N atoms.
[b] With diffuse *p* orbitals on the ligand O or N atoms.
[c] R(Å): equilibrium distance; θ: bond angle (Fig. 1), energy components as defined in the text.

For $Zn^{++}\cdots ImH$ and $Zn^{++}\cdots Im^{-}$, again the loss in Coulomb energy as θ increases is strong. But it is in part compensated for by a decrease of the exchange repulsion (as the nitrogen σ lone pair is moved away from Zn^{++}) and an increase in the E_{DEL} term, increase due mainly to a stronger polarization, as discussed above. $Zn^{++}\cdots Im^{-}$ is easier to bend than $Zn^{++}\cdots ImH$ because (due to the negative charge on Im^{-}) there is a somewhat smaller Coulombic energy loss as θ increases; furthermore the decrease of the exchange repulsion is much greater, a fact which can be ascribed to the more diffuse nature of the nitrogen σ lone pair in the anion; there is also a slight increase in the E_{DEL} term.

Finally, with $Zn^{++}\cdots OH^{-}$, we have a case where the optimum geometry is not determined solely by the Coulomb term but results from a balance, the Coulomb term favoring large θ (i.e. lone pair directionality) as well as the E_{DEL} term, which however changes very little, and the exchange repulsion favoring $\theta=0°$.

It must be stressed again [52, 53, 51] that the complex balance between the various components may very well be reversed in different complexes involving the same ligands with another cation. An interesting example is provided by a recent calculation on $H^{+}+OCO$ [54] which has shown that in the optimum geometry, the H–O–C angle is near 120° (i.e. $\theta=60°$) and the H–O distance is about 0.98 Å. This differs from our result on $Zn^{++}\cdots OCO$ where we find $\theta=0°$ strongly favored, and a Zn···O distance of 1.85 Å. It was tempting to speculate that the electrostatic potential of CO_2 at about 1 Å from O would be more negative at $\theta=60°$ than at $\theta=0°$ and that the reverse would be true at about 2.0 Å. Calculations of the electrostatic potential of CO_2 at $\theta=0°$ and $\theta=60°$ at distances from 1 to 6 a.u. (0.5 to 3.0 Å) show however that the potential is always more negative along the OCO axis ($\theta=0°$), so that the bent structure of $H^{+}\cdots OCO$ must probably be ascribed to the E_{DEL} component of the energy of that system.

3.3. Role of the d Orbitals in the Binding

In all the complexes studied here, there is to some extent mixing of the $3d\sigma$ AO of Zn^{++} with the σ lone pair of the donor; the mixing is strongest for CO_2 and Im^{-} (3/1) and quite weaker for OH^{-}, ImH, and OH_2. As noted in a recent study of ZnS [12], since both the bonding and antibonding MO's are occupied, one cannot expect that this mixing leads to a net bonding interaction. Hence one is justified in describing the $3d$ orbitals of zinc as core-like [12]. In all cases, population analysis shows that the "covalent component" of the $Zn^{++}\cdots$ligand binding arises essentially from interaction between the occupied σ lone pair of the ligand and the empty $4s$ and $4p\sigma$ orbitals of the cation.

Upon formation of the bond, all orbital energies of the ligand are lowered while those of the metal ion are raised (see Table 8 in Sect. 4). This is what one expects qualitatively since charge is transferred to Zn^{++} and since the strong positive charge of the cation must stabilize the orbitals of the ligand. Similar trends in the

molecular orbital energies of the electron donor and electron acceptor molecules upon hydrogen bond formation have been described [55].

3.4. Imidazole as a Ligand

In discussions of imidazole as a ligand [31], it is usually said that imidazole has a good basicity and π acceptor capability, which makes it intermediate between NH_3 (more basic, no π acceptor capability) and pyridine (less basic, better π acceptor). Stability constants for the first association of L to Zn^{++} in aqueous solutions, collected in Ref. [31], are $K_1 = 2.37$ for NH_3, 2.52 for ImH and 0.88 for pyridine. In this context one is led to conclude that the π acceptor ability of ImH overcompensates for its poorer basicity compared to that of NH_3.

Our data concerning Zn^{++} bonding in Table 5 allow the following comments: imidazole (and more so Im^-) is a very good σ donor, and weak π donor to zinc. π electron donation from ImH to zinc is in fact no greater than that from OH_2 to zinc. Of course, the Zn^{++} ion does not have high-lying occupied π orbitals which could participate in π-back donation to its ligand. However, calculations by Dedieu *et al.* [56, 57] on complexes in which imidazole is bound to a cobalt or to an iron ion show only a very slight (0.007 and 0.004 e) π back donation to the imidazole ring.

Our conclusion, shared by these authors, is that imidazole is neither a strong π donor nor a strong π acceptor.

However the imidazole complexes stand out for their very large π *charge shifts* (Table 5), due to their highly polarizable π system. We conclude that π electron polarizability, and not π electron donor or acceptor character, as well as strong σ donor capability, are the two important features of imidazole binding to metal ions. This conclusion receives support both from the detailed analysis of atomic population changes upon complex formation and from electron density difference plots.

The details of atomic population changes in $Zn^{++}\cdots$ImH upon complex formation are given in Fig. 2, for total, σ and π changes. The total population changes show a transfer to Zn and an accumulation of charge on N1, with global loss of charge from all other atoms. The π electron population changes are somewhat different: there is little π transfer to Zn, but a large accumulation of π charge on N1 and a smaller one on C5, at the expense of the three other atoms of the ring. The σ electron population changes show a large transfer to Zn, a charge accumulation on N1 and (less) on C4 and N3. This σ charge comes mostly from the hydrogen atoms. Population changes in $Zn^{++}\cdots Im^-$ are qualitatively similar and will not be discussed here.

A perhaps better image of the electron displacements upon complex formation is given by the electron density difference plots for $Zn^{++}\cdots$ImH presented in Fig. 4.

The π electron density difference plot (Fig. 4b) strikingly illustrates the large π polarization and weak π charge transfer: it shows a large accumulation of density

around N1 and a weak one on C5 and on Zn, and a charge depletion between Zn and N1 and on the C2, N3 and C4 atoms. The in-plane σ electron density difference map (Fig. 4a) has already been discussed. Let us note however that the patterns of charge density rearrangement around Zn and around N1, C2 and C5 are rather complex and do not appear in the population analysis. In particular the atomic populations (Fig. 2) do not show the striking electron density decrease in the σ lone pair of N1. Other charge density changes apparent from Fig. 4 (density increases on N3 and C4, decreases on the hydrogens) do appear in the atomic population changes of Fig. 2. On the whole, population changes in terms of charge shifts and transfers, and density difference plots complement each other nicely.

3.5. Water as a Ligand to Zinc

Zundel and Murr [38] have observed that Zn^{++} interacts more strongly with OH_2 than Mg^{++}, although the electric field at the O atom due to the cation should be stronger for Mg^{++}, due to its smaller radius. They conclude that $Zn^{++}\cdots OH_2$ bonding has a covalent component on top of the Coulombic interaction, which is lacking in $Mg^{++}\cdots OH_2$. They describe it as bonding between a Zn 3*d*, 4*s*, 4*p* hybrid and the oxygen lone pair.

We have made a calculation on $Mg^{++}\cdots OH_2$ using for Mg a basis set as close as possible in quality to that adopted for Zn^{++}. We find an equilibrium Mg···O distance of about 1.9 Å, a charge transfer of 0.148 e, $\Delta E = -91.6$ kcal/mole, $E_C = -99.2$ kcal/mole, $E_{EX} = 29.22$ kcal/mole and $E_{DEL} = -21.6$ kcal/mole.

Our $Zn^{++}\cdots OH_2$ calculation gives at the equilibrium distance of 1.89 Å a charge transfer of 0.207 e, $\Delta E = -104.2$ kcal/mole, $E_C = -115.9$ kcal/mole, $E_{EX} =$ 47.4 kcal/mole and $E_{DEL} = -35.6$ kcal/mole.

Although one should not attempt to make too quantitative a comparison, the results appear qualitatively reasonable: the exchange repulsion is greater for Zn^{++}, which has more electrons than Mg^{++}. Charge transfer is larger and the E_{DEL} term sensibly larger for Zn^{++} both in absolute value and as a percentage of the total calculated binding energy ($E_{DEL} = 34\%$ of ΔE for $Zn^{++}\cdots OH_2$, $E_{DEL} = 24\%$ of ΔE for $Mg^{++}\cdots OH_2$). All this points to a greater 'covalent character' of the $Zn^{++}\cdots OH_2$ interaction. We would not however describe it as interaction of the oxygen lone pair with a (3*d*, 4*s*, 4*p*) Zn hybrid AO. Detailed atomic orbital populations on zinc in $Zn^{++}\cdots OH_2$ show the following: $3d\sigma$ AO's loose 0.015 e while $3d\pi$ AO's gain 0.008 e. The main charge gain occurs in the previously empty 4*s* AO (0.119 e), 4*px* AO (0.075 e) and a little $4p\pi$ AO (0.015 e). Molecular orbital coefficients and atomic populations do show a slight $3d\sigma$–oxygen $2p\sigma$ mixing (in MO 12), but the largest mixing occurs in MO 18 (just below the *homo*) between the oxygen σ lone pair and an empty Zn 4*s*, $4p\sigma$ hybrid. The difference between Zn^{++} and Mg^{++} bonding to water may be simply due to the greater accessibility of the empty Zn 4*s* AO compared to the Mg 3*s* AO due to the imperfect shielding of the core by the 10*d* electrons in Zn^{++}: IP_2 of Zn = 17.89 eV while IP_2 of Mg = 15.03 eV [58].

4. Test of the Pseudopotential Method

The largest calculations presented here, on Zn^{++}···ImH, are already quite time-consuming. In view of investigating more realistic, and hence larger, model systems for the biochemical interactions of interest, it would be very useful to be able to utilize with a good degree of confidence *ab initio* valence-electron-only pseudopotential techniques. Among the pseudopotential methods recently proposed we have chosen one [21] which is based on parameters independent of the basis functions used in the calculation, and which has been included in the program IBMOLH in our laboratory by N. Gresh. In order to facilitate the comparison between the full computation and pseudopotential one, we have chosen to use the valence part of our basis set (Table 1), instead of using valence basis functions especially optimized for the pseudopotential used. Specifically, the Zn 1*s*, 2*s*, 2*p*, 3*s* and 3*p* shells, the nitrogen, carbon and oxygen 1*s* shells were treated as core electrons, simulated by Topiol's pseudopotentials [22]. Numerical experiment showed that only four of the five functions used to describe the 1*s* orbital of oxygen could be deleted from the basis function if a good description of the innermost valence molecular orbital was to be achieved. The final basis sets are: Zn 4*s*, 1*p*, 4*d*→ 3*s*, 1*p*, 3*d*; O, N: 3*s*, 4*p*→ 3*s*, 3*p*; C 3*s*, 3*p*→ 3*s*, 2*p*.

Table 7. Computed binding energies to Zn^{++} of various ligands at various distances and angles. Pseudopotential results

Complex	R(Å)	θ, Degree	ΔE[a]	$\delta(\Delta E)$[b]
Zn^{++}···OCO[c]	1.80	0		0.7
	1.85	0	−77.2	0.0
	1.90	0		0.4
	2.50	0	−47.6	29.6
Zn^{++}···OH_2	1.80	0		1.4
	1.89	0	−103.0	0.0
	2.0	0		2.4
	1.89	15		1.2
	1.89	30		4.7
	1.89	60		20.2
	1.89	90		49.7
Zn^{++}···ImH	2.0	0	−165.8	[d]
Zn^{++}···Im^-	1.85	0	−367.8	[d]
Zn^{++}···OH^-	1.55	0°		10.4
	1.65	0		1.7
	1.70	0	−413.0	0.0
	1.75	0		3.0

[a] Binding energy (kcal/mole) of Zn^{++}···L computed as $E(Zn^{++}$···L)–$E(Zn^{++})$–E(L).

[b] $\delta(\Delta E)$: energy with respect to optimum geometry (kcal/mole).

[c] No diffuse p functions were used on the neutral CO_2 ligand.

[d] No geometry optimization was made for this complex with the pseudopotential method.

Results of our pseudopotential calculations are given in Tables 7 to 9.

Comparing Tables 3 and 7, we find that the pseudopotential calculations reproduce very well the optimum geometries and that the bonding energies are identical within 1 to 3 kcal/mole, a very small percentage of the total binding energy.

Even in non-equilibrium geometries (at large R or at $\theta \neq 0°$) the binding energies remain very close to the all-electrons values.

Orbital energies are compared in Table 8 for several systems. The all-electrons and pseudopotential molecular orbital energies agree to about 1 to $2 \cdot 10^{-2}$ a.u. for the lowest valence MO's (O 2*s*, Zn 3*d* etc.) and even to 1 to 5.10^{-3} a.u. for the highest valence MO's. The population analysis (Tables 5 and 9) gives results which are

Table 8. Comparison of valence orbital energies ($-\varepsilon$, in hartree units) in all electrons and pseudopotential calculations

Compound	Full	Pseudo	Compound	Full	Pseudo
Zn^{++}	1.5120	1.5360	$Zn^{++}\cdots OH_2$	1.8704	1.8604
			$R=1.89$ Å	1.4038	1.4250
OH_2	1.3607	1.3504		1.3965	1.4155
	0.7296	0.7289		1.3965	1.4149
	0.5771	0.5750		1.3957	1.4122
	0.5176	0.5173		1.3946	1.4122
				1.2338	1.2353
OH^-	0.8931	0.8827		1.1573	1.1560
	0.2401	0.2387		1.0408	1.0422
	0.1087	0.1090			
	0.1087	0.1090	$Zn^{++}\cdots OH^-$	1.4524	1.4455
			$R=1.70$ Å	1.1293	1.1473
CO_2	1.5445	1.5246		1.1288	1.1456
	1.5023	1.4933		1.1288	1.1456
	0.7727	0.7742		1.1270	1.1368
	0.7294	0.7287		1.1270	1.1368
	0.7293	0.7287		0.8431	0.8440
	0.7293	0.7276		0.6635	0.6687
	0.5327	0.5333		0.6635	0.6687
	0.5327	0.5333			
			$Zn\cdots OCO$	1.9735	1.9613
			$R=1.85$ Å	1.9049	1.8941
				1.4319	1.4549
				1.4007	1.4246
				1.4007	1.4246
				1.4001	1.4208
				1.4001	1.4208
				1.2713	1.2767
				1.1519	1.1555
				1.1519	1.1555
				1.1176	1.1170
				0.9501	0.9522
				0.9501	0.9522

Table 9. Mulliken population analysis (in 10^{-3} electron) pseudopotential results (equilibrium geometries)

	Charge transfer				Charge shift		
Ligand[a]	Total	σ	π	$\%\pi$	Total	σ	π
CO_2	203	162	41	20	287	—	291
H_2O	241	219	22	11	101	123	—
ImH	446	426	20	4	305	21	343
Im^-	658	616	42	6	190	—	320
OH^-	509	372	137	27	—	—	—

[a] With diffuse *p* orbitals on ligand O or N atoms except for CO_2.
Charge transfer and charge shift as defined in the text.

qualitatively in agreement with those of the all-electrons calculation. We find however that the pseudopotential calculation with the present basis sets overestimates the amount of charge transferred to the Zn^{++} cation. Further examination shows that it is the σ charge transfer that is exaggerated. Conversely, the total charge shifts are usually underestimated by the pseudopotential method, which indicates that the total charge rearrangement within the complex are roughly correctly described. In any event the qualitative conclusions which we have made from the full SCF population analysis could equally be made from the pseudopotential results.

The weaker performance for the orbital energies of the lowest valence MO's, and the fact that we had to keep one of the five "1*s*" primitives for oxygen, nitrogen and carbon, stress the following point: the Gaussian basis sets which we used have not been designed specifically to be separable into core and valence regions, and the "1*s*" basis functions contribute to some extent also to the 2*s* AO [59]. The use of basis sets specifically designed for the pseudopotential calculation may be preferable in the future, although one will lose the ability to compare in detail with an all-electrons calculation.

In conclusion, we find that even with the present basis sets, which have not been tailored for the pseudopotential, the valence electron calculations lead to excellent agreement with *ab initio* calculations and may be used with confidence on larger systems where all-electrons calculations might be too costly. Agreement is excellent for binding energies and geometry search, quite good for orbital energies, and at least qualitatively satisfying for population analysis.

Acknowledgements. We would like to thank D. Perahia for his help in the programming of the energy decomposition scheme, and B. Sarkar for many fruitful discussions while he was Visiting Professor in our Institute.

This research was supported by the National Foundation for Cancer Research (USA) and by ATP 2646 of the CNRS. We thank Professor Albert Szent-Gyorgyi for stimulative encouragements and discussions.

References

1. Dunn, M. F.: Structure and bonding **23**, 61 (1976)
2. Lindskog, S., Henderson, L., Kannan, K. K., Liljas, A., Nyman, P. O., Strandberg, B., in: The enzymes, vol. 5, third edn, Boyer, P. ed., p. 587. New York: Academic Press 1971
3. Lipscomb, W. N., Hartsuck, A., Recke, G. N., Quiocho, F. A., Bethge, P. W., Ludwig, M. L., Steitz, T. A., Muirhead, H., Coppola, C.: Brookhaven Symp. Biol. **21**, 24 (1968)
4. Matthews, B. W., Jansonius, J. N., Colman, P. M., Schoenborn, B. P., Dupourque, D.: Nature, New Biol. **238**, 37 (1972)
5. Brändén, C. I., Eklund, H., Nordström, B., Boiwe, T., Söderlund, G., Zeppezauer, E., Ohlsson, I., Åkeson, Å.: Proc. Natl. Acad. Sci. U.S. **70**, 2439 (1973)
6. Slater, J. P., Mildvan, A. S., Loeb, L. A.: Biochem. Biophys. Res. Commun. **44**, 37 (1971)
7. Springgate, C. F., Mildvan, A. S., Abramson, R., Engle, J. L., Loeb, L. A.: J. Biol. Chem. **248**, 5987 (1973)
8. Scrutton, M. C., Wu, C. W., Goldthwait, D. A.: Proc. Natl. Acad. Sci. U.S. **68**, 2497 (1971)
9. Auld, D. S., Atsuya, I., Campino, C., Valenzuela, P.: Biochem. Biophys. Res. Commun. **69**, 548 (1976)
10. Vallee, B. L.: Experientia **33**, 600 (1977)
11. Demoulin, D., Pullman, A., Sarkar, B.: J. Am. Chem. Soc. **99**, 8498 (1977)
12. Hinchliffe, A., Dobson, J. C.: Theoret. Chim. Acta (Berl.) **39**, 211 (1975)
13. Yarkony, D. R., Schaeffer III, H. F.: Chem. Phys. Letters **15**, 514 (1972)
14. Ratner, M., Moskowitz, J. W., Topiol, S.: Chem. Phys. Letters **46**, 495 (1977)
15. Bancroft, G. M., Creber, D. K., Ratner, M. A., Moskowitz, J. W., Topiol, S.: Chem. Phys. Letters **50**, 233 (1977)
16. Demoulin, D., Fischer-Hjalmars, I., Henriksson-Enflo, A., Pappas, J. A., Sundbom, M.: Intern. J. Quantum Chem., in press.
17. Apleton, D. W., Sarkar, B.: Proc. Natl. Acad. Sci. US **69**, 2422 (1974)
18. Kannan, K. K., Petef, M., Fridborg, K., Cid-Dresdner, H., Lövgren, S.: FEBS Letters **73**, 115 (1977)
19. Dreyfus, M., Pullman, A.: Theoret. Chim. Acta (Berl.) **19**, 20 (1970)
20. Mulliken, R. S.: J. Chem. Phys. **23**, 1833 (1955)
21. Melius, C. F., Goddard III, W. A., Kahn, L. R.: J. Chem. Phys. **56**, 3342 (1972)
22. Topiol, S., Moskowitz, J. W., Melius, C. F., Newton, M. V., Jaffri, J.: Courant Institute of Mathematical Science, ERDA Research and Development Report (COO-3077-105)
23. Kistenmacher, H., Popkie, H., Clementi, E.: J. Chem. Phys. **59**, 5842 (1973)
24. Diercksen, G. H. F., Kraemer, W. P., Roos, B. O.: Theoret. Chim. Acta (Berl.) **36**, 249 (1975)
25. Woodin, R. L., Houle, F. A., Goddard III, W. A.: Chem. Phys. **14**, 461 (1976)
26. Kochanski, E.: private communication
27. Martinez-Carrera, S.: Acta Cryst. **20**, 783 (1966)
28. Jönsson, B., Karlstrom, G., Wennerström, H.: Chem. Phys. Letters **30**, 58 (1975)
29. Sutton, L. E.: Tables of interatomic distances. Chem. Soc. Spec. Publ. **18** (1965)
30. Freeman, H. C.: in Inorganic biochemistry, vol. 1, Eichhorn, G. L. ed., p. 121. Amsterdam: Elsevier 1973
31. Sundberg, R. J., Martin, R. B.: Chem. Rev. **74**, 471 (1974)
32. Roos, B., Veillard, A., Vinot, G.: Theoret. Chim. Acta (Berl.) **20**, 1 (1971)
33. Roos, B., Siegbahn, P.: Theoret. Chim. Acta (Berl.) **17**, 209 (1970)
34. Dunning, T. H.: J. Chem. Phys. **53**, 2823 (1970)
35. Whitman, D. R., Hornback, C. J.: J. Chem. Phys. **51**, 398 (1969)
36. Brauman, J. I., Blair, L. K.: J. Am. Chem. Soc. **92**, 5986 (1970)
37. Veillard, H., Demuynck, J., Veillard, A.: Chem. Phys. Letters **33**, 221 (1975)
38. Zundel, G., Murr, A., in: Metal ligand interactions in organic chemistry and biochemistry, part 2, p. 265, Pullman, B., Goldblum, N. eds. Dordrecht, Holland: D. Reidel Publ. Comp. 1977
39. Kannan, K. K.: private communication
40. Montgomery, H., Lingafilter, E. C.: Acta Cryst. **16**, 748 (1963)
41. Osipov, O. A., Simonov, A. M., Minkin, V. I., Garneskii, A. D.: Dokl. Akad. Nauk. SSSR **137**, 1374 (1961)

42. Nelson, R. D., Lide, D. R., Maryotte, A. A.: U.S. Dept. of Commerce, Natl. Bur. Stand. NSRDS-NBS 10 (1967)
43. Budenholzer, F. D., Gislason, E. A., Jorgensen, A. D., Sachs, J. G.: Chem. Phys. Letters **47**, 429 (1977)
44. Kitaura, K., Morokuma, K.: Intern. J. Quantum Chem. **10**, 325 (1976)
45. Dreyfus, M., Maigret, B., Pullman, A.: Theoret. Chim. Acta (Berl.) **17**, 109 (1970)
46. Kollman, P. A., Allen, L. C.: J. Chem. Phys. **52**, 5085 (1970)
47. Russeger, P., Schuster, P.: Chem. Phys. Letters **19**, 245 (1973)
48. Schuster, P., Marius, W., Pullman, A., Berthod, H.: Theoret. Chim. Acta (Berl.) **40**, 323 (1975)
49. Umeyama, H., Morokuma, K.: J. Am. Chem. Soc. **98**, 7208 (1976)
50. Kollman, P. A.: J. Am. Chem. Soc. **94**, 1837 (1972)
51. Kollman, P.: J. Am. Chem. Soc. **99**, 4875 (1977)
52. Perahia, D., Pullman, A., Pullman, B.: Theoret. Chim. Acta (Berl.) **43**, 207 (1977)
53. Pullman, A., Armbruster, A. M.: Theoret. Chim. Acta (Berl.) **45**, 249 (1977)
54. Green, S., Schor, H., Siegbahn, P., Thaddeus, P.: Chem. Phys. **17**, 479 (1976)
55. Kollman, P., Allen, L. C.: J. Am. Chem. Soc. **93**, 4991 (1970)
56. Dedieu, A., Rohmer, M. M., Veillard, A.: J. Am. Chem. Soc. **98**, 3717 (1976)
57. Dedieu, A., Rohmer, M. M., Veillard, A., in: Metal ligand interactions in organic chemistry and biochemistry part 2, p. 101. Pullman, B., Goldblum, N. eds. Dordrecht, Holland: D. Reidel Publ. Comp. 1977
58. Cotton, F. A., Wilkinson, G.: Advanced inorganic chemistry, third edn. New York: Interscience Publishers 1972
59. Gresh, N., Pullman, A.: Theoret. Chim. Acta (Berl.) in press

Received March 13, 1978